ACS OMEGA

Article

Cite This: ACS Omega 2018, 3, 2220−2229

Phytochemicals as Dynamic Surface Ligands To Control Nanoparticle−Protein Interactions

Amanda N. Abraham,[†] Tarun K. Sharma,[†] Vipul Bansal,*[,†] and Ravi Shukla*[,†,‡]

[†]Ian Potter NanoBioSensing Facility, NanoBiotechnology Research Lab (NBRL), School of Science, and [‡]Centre for Advanced Materials & Industrial Chemistry, School of Science, RMIT University, GPO Box 2476 V, Melbourne, Victoria 3001, Australia

Supporting Information

ABSTRACT: The rapid formation of the protein corona on to the nanoparticle (NP) surface is the key that confers biological identity to NPs and subsequently dictates their fate both in vitro and in vivo. Despite significant efforts, the inability to control the spontaneous interaction of serum proteins with the administered NPs remains a major constraint in clinical translation of nanomedicines. The ligands present on the NP surface offer promise in controlling their biological interactions; however, their influence on the NP−protein interaction is not well-understood. The current study investigates the potential of phytochemical-capped silver nanoparticles (AgNPs) toward allowing a control over NP interactions with the human serum albumin (HSA), the most abundant protein in the biological fluids. Specifically, we demonstrate the ability of curcumin (Cur) and epigallocatechin-3-gallate (EGCG) to independently act as reducing agents to produce phytochemical-capped AgNPs that show biologically desirable interactions with HSA. The key finding of our study is that the phytochemical-capped AgNPs initially interact with HSA more strongly compared to the citrate-stabilized AgNPs; however, the resultant NP−HSA complexes are less stable in the case of the former, which causes a lesser degree of changes in the protein conformation during interactions. Further, the choice of the phytochemical allows control over NP−HSA interactions, such that Cur- and EGCG-capped AgNPs interacted with HSA in a static versus dynamic manner, respectively. The diversity of the functional groups present in natural phytochemicals and their potential as in situ capping ligands during synthesis offer new opportunities in controlling the interactions of NPs with complex biological fluids, with implications in nanodiagnostics and nanomedicine.

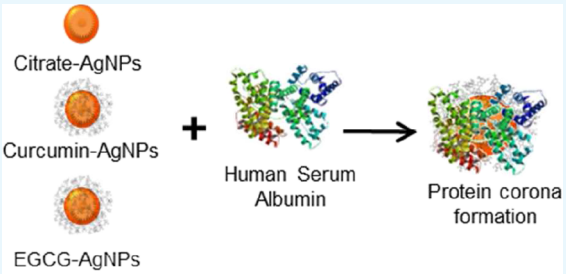

Phytochemical-coated silver nanoparticles cause lesser degree of changes in serum protein conformation during protein corona formation.

INTRODUCTION

The unique physicochemical and broad spectrum antibacterial and antifungal properties of silver nanoparticles (AgNPs) have made them one of the most incorporated nanomaterials in the consumer and medical products to date.[1,2] However, on administering these NPs into the blood stream, they first come into contact with proteins found in the plasma.[3] These plasma proteins readily interact with the surface of the NPs forming a protein corona (PC).[4] This initial interaction between the NPs and plasma proteins changes the properties of the NPs, and as such, this has remarkable impact on altering the mechanism of NP interaction with the target organs.[5] Hence, distribution and biological responses of the NPs in the body are dictated by this PC because this altered configuration of NPs is what that is perceived when the NPs first come in contact with the target cells.[4,6,7] The NPs, in turn, can also change the conformation of the plasma proteins they interact with, possibly altering the function of these proteins.[1] Hence, when considering the use of NPs for in vivo purposes, it is important to understand and control these interactions of NPs with proteins in the blood stream.

Albumins are the most abundant proteins found in the human serum, at a concentration of 769 μM/L.[8] Human serum albumin (HSA) contains 585 amino acid residues, and it serves as an important carrier for many substances such as fatty acids, bilirubins, hormones, and exogenous and endogenous ligands.[9] Because HSA possesses so many important physiological functions, any change to its structure can prove detrimental to its normal functioning in the body.[1,10,11] Hence, it is important to study the interaction of NPs with this protein. In particular, HSA contains a single tryptophan (Trp-214) residue in the hydrophobic cavity of its sub-domain IIA (Sudlow I). This Trp residue is capable of producing strong intrinsic fluorescence and therefore serves as an excellent reporter for ligand binding and conformational studies.[1,12]

Notably, while there are some studies that have utilized human serum or simulated complex biological environments,[13,14] most studies that have looked at NP−protein interactions have utilized bovine serum albumin (BSA)[3,6,15−18]

Received: November 28, 2017
Accepted: February 5, 2018
Published: February 22, 2018

DOI: 10.1021/acsomega.7b01878
ACS Omega 2018, 3, 2220−2229

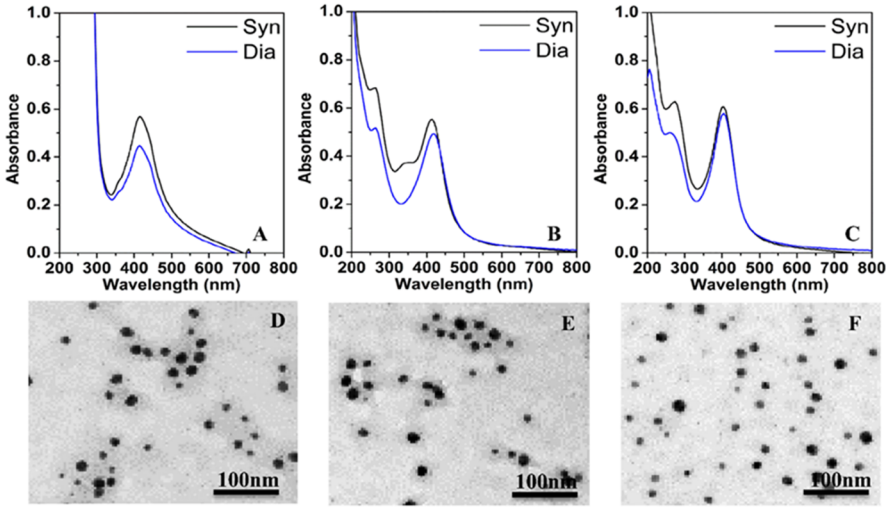

Figure 1. UV−vis absorbance spectra (A−C) of as-synthesized (Syn) and post-dialysis (Dia) nanoparticles and corresponding post-dialysis TEM images (D−F) of Ct-AgNPs (A,D), Cur-AgNPs (B,E), and EGCG-AgNPs (C,F).

instead of HSA. However, one important difference between BSA and HSA is the presence of two tryptophan residues in BSA, whereas HSA has a single unique tryptophan residue.[12,19] Owing to this inherent difference, these two proteins may show different binding interactions with NPs. For instance, Gelamo and Tabak[19] noted that in the presence of various ionic surfactants, BSA evinced fluorescence quenching, whereas HSA led to an enhancement of the fluorescence with the same ionic surfactants. Manivel and Anandan[2] also observed that BSA can exhibit higher binding with NPs than HSA. This supports that BSA is not a reliable substitute for HSA, especially when employing fluorescence for fundamental interaction studies. As such, in contrast to a serum protein of bovine origin, HSA offers a more appropriate platform to study and understand the NP interactions in the human context. Hence, our current study focuses on studying the interaction of HSA with NPs to obtain insights into the likely fate of NPs in the human blood/serum.

On the other hand, the NP surface characteristics, viz., the biomolecules or phytochemicals present on the surface, may also affect the degree and type of serum protein interactions. Isolated phytochemicals, such as curcumin,[20] epigallocatechin-3-gallate (EGCG),[21] and various flavonoids,[22] have been observed to show interactions with serum. However, the study of the interaction of phytochemical-coated NPs remains elusive. It is important to study the direct interaction of phytochemical-coated NPs with serum proteins, as it is not uncommon for the functional groups of the phytochemicals to be modified during the process of NP synthesis and capping.[23] This altered structure of phytochemical bound onto the NP surface could in turn influence the mode of interactions with serum proteins. It is also a focus of our current study to understand how this change in the phytochemical structure might affect the interaction of these NPs with proteins in the blood. To obtain insights into these fundamental questions, we utilize curcumin and EGCG phytochemicals found in turmeric and green tea, respectively, to synthesize AgNPs and elucidate their physicochemical interactions with HSA. We chose curcumin and EGCG as ligands in the current study, as these two phytochemicals have been actively investigated for their therapeutic potential. For instance, EGCG has been recently exploited as a ligand to selectively target Laminin-67 receptor, a protein overexpressed on the surface of prostate cancer cells.[24] The EGCG functionalization on the surface of gold NPs led to selective uptake of these NPs into cancer cells which could be employed for therapeutic purpose. Similarly, the use of curcumin-based nanoformulations has been actively proposed for a number of biomedical applications ranging from therapy of cancer to cardiovascular diseases, Alzheimer's disease, inflammations, and neurological disorders.[25]

RESULTS AND DISCUSSION

Synthesis and Characterization of Phytochemical-Coated AgNPs. Phytochemical-coated AgNPs were synthesized and characterized by UV−vis absorbance spectroscopy, transmission electron microscopy (TEM), dynamic light scattering (DLS), and zeta-potential measurements. Figure 1A−C compares the UV−vis absorbance spectra of the as-synthesised AgNPs using different reducing agents and those obtained after dialysis to remove potentially unutilized precursors. AgNPs obtained using citrate, curcumin, and EGCG as reducing agents have been referred as Ct-AgNPs, Cur-AgNPs, and EGCG-AgNPs throughout this study. The as-synthesized AgNPs display characteristic surface plasmon resonance (SPR) bands ca. 405−416 nm (408 nm for Ct-AgNPs, 416 nm for Cur-AgNPs, and 406 nm for EGCG-AgNPs).[3,26] Additional absorption features are observed at ca. 260−280 nm only in the case of phytochemical-stabilized NPs. Supporting Information Figure S1 shows the absorbance features of curcumin at 263 and 417 nm[27] and EGCG at 235 and 273 nm.[28] Hence, the 263 nm peak for Cur−AgNPs and the 273 nm peak for EGCG-AgNPs can be ascribed to the electronic transitions from the benzene ring present in these phytochemicals. Subsequent to the dialysis performed on these NPs, the free phytochemicals are removed, leading to a decrease in the intensity of the absorption peaks corresponding to these phytochemicals. The high intensity absorption peak observed ca. 209 nm in the case of Ct-AgNPs possibly stems from the citrate on the NPs because trisodium citrate shows an absorption band at 209 nm (Supporting Information Figure S1).[29] The resulting absorbance features seen in the UV range of the spectra after dialysis stem from the citrate and phytochemicals firmly bound to the surface of AgNPs.

DOI: 10.1021/acsomega.7b01878
ACS Omega 2018, 3, 2220−2229

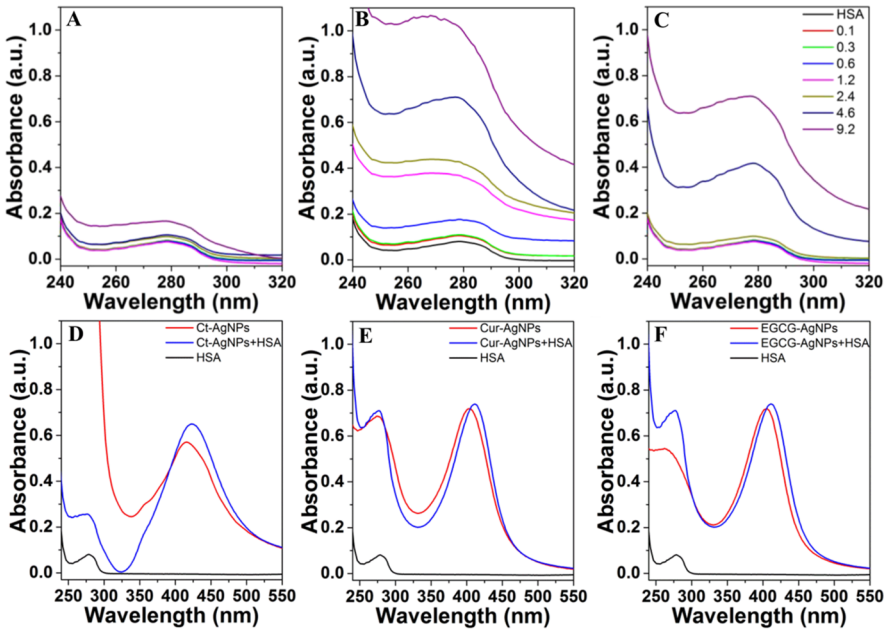

Figure 2. UV−vis absorption spectra in (A−C) depicting interactions of a fixed concentration of HSA (3 μM) with an increasing concentration of AgNPs (0−9.2 μM) in the HSA absorption region. HSA in the figure corresponds to the equivalent concentration of HSA without nanoparticles. (D−F) depict changes in the SPR absorbance of AgNPs (1.2 μM) on exposure to HSA (3 μM). (A,D) Ct-AgNPs, (B,E) Cur-AgNPs, and (C,F) EGCG-AgNPs.

The phytochemical-coated AgNPs as well as Ct-AgNPs were of narrow size distribution with a mean diameter of 10−20 nm, as confirmed by TEM (Figure 1D−F). Previous studies have noted that NPs <50 nm in diameter are readily internalized into cells,[30] suggesting that AgNPs used in the current study are in an appropriate size range for potential biological applications. The hydrodynamic diameters for Ct-AgNPs, Cur-AgNPs, and EGCG-AgNPs were recorded to be 55.6, 44.8, and 61.5 nm, respectively; and the corresponding zeta potentials were −25.9, −41.3, and −38.9 mV (Supporting Information, Table S1).

As a preliminary method of determining the interaction of HSA with AgNPs, the changes in the DLS and zeta potential of NPs were monitored in the presence and absence of HSA. The hydrodynamic diameters of AgNPs increase in the presence of HSA, accompanied with a concomitant decrease in the zeta potential (Supporting Information, Table S1). The Ct-AgNPs and EGCG-AgNPs show 10% increase in the hydrodynamic diameter in the presence of HSA, while Cur-AgNPs show a 30% increase. This indicates that Cur-AgNPs have a greater degree of interactions with HSA over the other two NP types. Brewer et al.[16] have noted that a decrease in the zeta potential indicates the binding of BSA to the surface of the NPs. In the current case, we observe that zeta potentials of all the three NP systems decrease on exposure to HSA, indicating that HSA binds to the surface of all three AgNPs forming a PC. The mechanism of these interactions is investigated further below.

Absorption Characteristics of AgNP Interactions with HSA. An increase in the absorption intensity of serum albumins with the increasing NP concentration has been attributed to a complex formation between these proteins and NPs and has been used as an indicator of the type of interactions between NPs and serum proteins.[1,3,11] As such, the interaction of a fixed amount of HSA with increasing concentrations of different AgNPs was initially investigated by monitoring the absorption features of HSA at ca. 279 nm. The results in Figure 2A−C show an increase in the intensity and blue shift in the HSA peak at 279 nm with the increasing AgNPs concentration beyond a certain minimal concentration threshold. This suggests the possibility of ground state complex formation between AgNPs and HSA because dynamic collisions only affect the excited states of the molecules and have no effect on the absorption spectra.[15] Similar effects of NPs on HSA absorption have been previously observed. Overall, the increase in the intensity of these interactions is significantly greater with phytochemical-coated AgNPs over Ct-AgNPs, and Cur-AgNPs show stronger interactions with HSA over EGCG-AgNPs. These observations, coupled with the DLS and zeta potential studies (Supporting Information Table S1), suggest that the phytochemical surface coating on AgNPs plays a significant role in influencing their interaction with serum proteins.

To further assess whether binding of HSA to the surface of AgNPs causes any NP aggregation, the SPR absorption features of AgNPs at c.a. 400 nm were also monitored in the presence of HSA (Figure 2D−F). The SPR peaks observed at 412 nm (Cur-AgNPs) and 406 nm (EGCG-AgNPs) marginally red-shifted to 413 and 412 nm, respectively, while the 416 nm Ct-AgNPs peak showed no significant change. The red shifts in the SPR peaks of the NPs indicate an increase in the overall NP hydrodynamic size, which further supports the DLS and zeta potential measurements (Supporting Information Table S1); because of phytochemical binding, the hydrodynamic diameter of AgNPs increases without causing NP aggregation.

Fluorescence Characteristics of AgNPs Interaction with HSA. The Trp-214 residue in HSA is highly sensitive to the changes in its microenvironment, thereby providing the intrinsic fluorescence emission of Trp as a good indicator of HSA interactions with other species.[31] Quenching or decrease in the fluorescence intensity may indicate a variety of interactions such as molecular rearrangement, collisional quenching, or ground state complex formation.[3,7] HSA showed an emission band at 346 nm on excitation at 295 nm, while AgNPs showed no fluorescence emission at this wavelength,

DOI: 10.1021/acsomega.7b01878
ACS Omega 2018, 3, 2220−2229

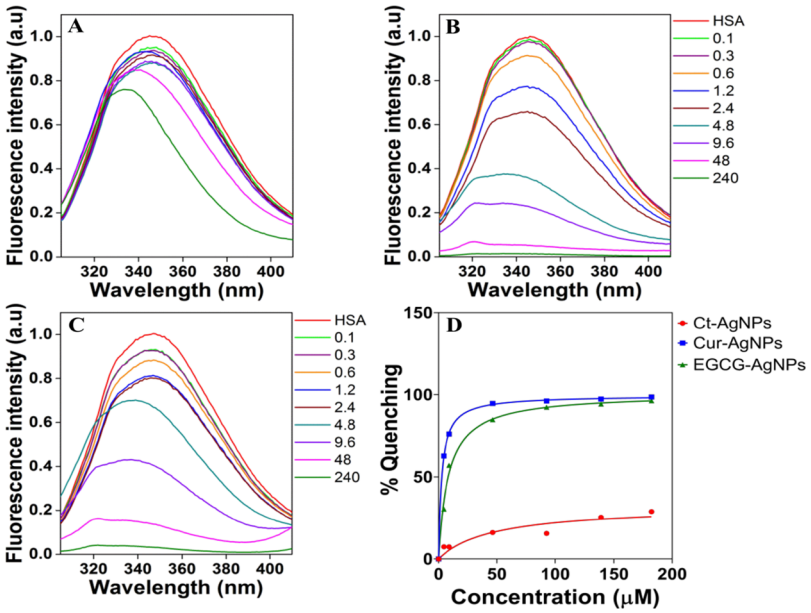

Figure 3. Fluorescence emission spectra in (A–C) depicting interactions of a fixed concentration of HSA (3 μM) with an increasing concentration of AgNPs (0–240 μM). HSA in the figure corresponds to the equivalent concentration of HSA (3 μM) without nanoparticles. (D) Apparent dissociation constants as obtained using nonlinear regression fits in GraphPad Prism 7.02 (GraphPad, La Jolla, CA, USA). (A) Ct-AgNPs, (B) Cur-AgNPs, and (C) EGCG-AgNPs.

indicating the absence of overlapping fluorescence spectra from the AgNPs (Figure 3). The HSA concentration was maintained constant at 3 μM, whereas the AgNP concentration was varied between 0 and 240 μM. These concentrations were chosen to mimic a variety of potential NP exposure scenarios, such that either the protein concentration is up to 30 times greater than that of the AgNPs or the AgNP concentration is 80 times greater than the protein concentration.

As shown in Figure 3A–C, in the presence of increasing concentrations of AgNPs, the Trp fluorescence was quenched in a NP concentration-dependent manner, with the largest degree of quenching caused by Cur-AgNPs, followed by EGCG-AgNPs and the least quenching observed with Ct-AgNPs. Because the efficiency of quenching depends on the proximity of the quencher to the fluorophore,[17] these results indicate that the AgNPs (quencher in the current case) bind to the HSA molecule (fluorophore in the current case) at or near its Trp residue in the subdomain IIA. Another interesting observation is an increasing blue shift in the fluorescence spectra of HSA with the increasing AgNP concentration. This shift in the fluorescence emission indicates a concentration-dependent effect of AgNPs on HSA, such that its chromophore (Trp residue) has been brought into a more hydrophobic surrounding.[1,11,32] To validate the role of the hydrophobic environment on blue shifts of HSA fluorescence signatures, we performed additional experiments, wherein a fixed amount of HSA in the phosphate buffer was independently exposed to increasingly higher concentrations (v/v wrt water) of less polar solvents such as methanol and ethanol. It is clear from Figure S2 (Supporting Information) that the hydrophobic environment leads to the blue shift in the HSA fluorescence peaks. Another interesting observation was that HSA fluorescence increased in the presence of a nonpolar environment. This increase in fluorescence with the alcohols could be due to the change in the protein structure, exposing the tryptophan molecule; however, with the AgNPs, this was not observed because of interactions of the AgNPs at or near the tryptophan. This supports our findings that the blue shift is due to the change in the hydrophobicity of the protein structure. Overall, these results signify that the AgNPs are capable of altering the structure of the HSA molecules.

From the fluorescence data, the dissociation constants (K_d) of HSA–AgNP interactions were calculated to determine the affinity of AgNPs with HSA (Figure 3D).[26] It is clear that the affinity of HSA toward Cur-AgNPs is the highest with a K_d of 2.9 μM, followed by EGCG-AgNPs (8.55 μM) and Ct-AgNPs (28.99 μM). In particular, Cur-AgNPs and EGCG-AgNPs show 10 and 3 times higher affinity toward HSA over Ct-AgNPs. These high affinities for Cur-AgNPs and EGCG-AgNPs to HSA are similar to the affinity observed with polyethylene glycol and glucose coated FePt NPs to HSA,[33−35] while the Ct-AgNPs are closer to the low affinity observed with polyacrylic acid-coated CdSe/ZnS NPs.[33,34] This supports that the nature of the capping agent over the NP surface plays a significant role in determining their interactions with serum proteins. Notably, while quenching of fluorescence emission during NP–protein interactions has been previously observed,[1−3,11,15,31] these studies have been restricted to studying a single type of NP, without considering the role of the surface corona.

It is acknowledged that free curcumin and EGCG molecules are known to show a phytochemical concentration-dependent increase in HSA fluorescence quenching.[36,37] However, interactions of pristine phytochemicals with HSA lead to red shifts in the fluorescence emission, which is indicative of shifts toward a more polar environment.[37] This is in contrast to phytochemical-coated AgNPs in the current case, where a blue shift (shifts toward a more nonpolar environment) in fluorescence emission is observed. Further, it was previously noted[38] that the hydroxyl groups on the galloyl moiety and on the B-ring of pristine EGCG are responsible for interactions with HSA. In the current case involving NPs, if the FTIR spectra of the Cur-AgNPs and EGCG-AgNPs are considered (Supporting Information Figure S3), a change in the phenolic groups of the phytochemicals on the surface of the AgNPs is

DOI: 10.1021/acsomega.7b01878
ACS Omega 2018, 3, 2220–2229

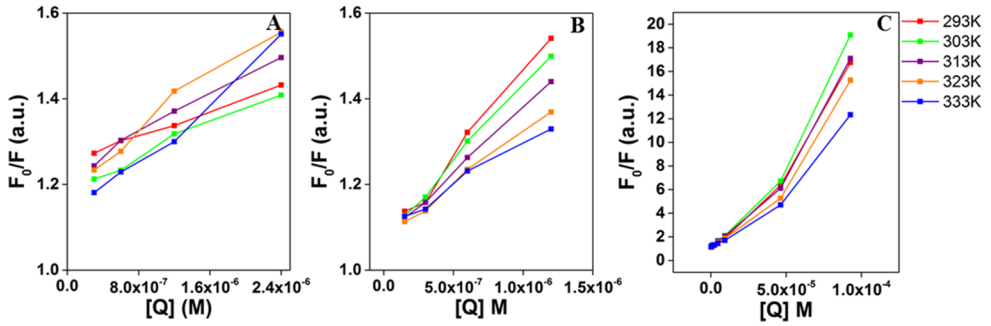

Figure 4. Stern–Volmer plots for (A) Ct-AgNPs, (B) Cur-AgNPs, and (C) EGCG-AgNPs at different temperatures.

Table 1. Stern–Volmer Constants and Thermodynamic Parameters for Cur-AgNPs

temperature (K)	K_{SV} (10^4 M^{-1})	k_q ($\times10^{13}$ M^{-1} s^{-1})	K ($\times10^3$ M^{-1})	$\Delta G°$ (kJ mol^{-1})	$\Delta H°$ (kJ mol^{-1})	$\Delta S°$ (J mol^{-1} K^{-1})
293	33.49	3.35	4.80	−54.02	81.75	184.63
303	40.03	4.00	3.13	−17.80	44.29	58.89
313	35.91	3.59	1.38	17.22	9.22	−54.99
323	30.64	3.06	0.43	51.16	−23.67	−158.45
333	24.92	2.49	0.11	84.11	−54.59	−252.74

Table 2. Stern–Volmer Constants and Thermodynamic Parameters for EGCG-AgNPs

temperature (K)	K_{SV} (10^4 M^{-1})	k_q ($\times10^{13}$ M^{-1} s^{-1})	K ($\times10^3$ M^{-1})	$\Delta G°$ (J mol^{-1})	$\Delta H°$ (kJ mol^{-1})	$\Delta S°$ (J K^{-1} mol^{-1})
293	15.04	1.50	7.53	−4.25	5.02	14.53
303	16.16	1.62	12.36	−2.07	2.72	6.83
313	18.42	1.84	14.27	0.05	0.57	−0.15
323	16.38	1.64	14.74	2.10	−1.44	−6.49
333	14.39	1.44	6.62	4.08	−3.34	−12.27

observed. This supports the fact that the chemical structures of phytochemicals change during reduction of Ag^+ ions and simultaneous surface capping of AgNPs. Therefore, it is not surprising that the interaction of phytochemical-coated AgNPs with HSA is not necessarily the same as the previously observed interaction of pristine phytochemicals with serum proteins. The authors recommend caution in making generalized predictions toward biological applicability of nanomaterials with a similar inorganic core but different surface cappings, or predicting the biological response of nanomaterials solely on the basis of the properties of pristine capping agents.

Fluorescence Quenching Mechanism. An interaction between a fluorophore and a quencher may undergo one of the two types of quenching mechanisms, viz., dynamic (or collisional) quenching and static quenching (or complex formation). Dynamic quenching occurs when a fluorophore in an excited state is deactivated when it remains in contact with the quencher, whereas static quenching occurs when the quencher and the fluorophore form a nonfluorescent ground state complex.[3,26] These two types of quenching can be differentiated by studying the interactions as a function of temperature. In a dynamic quenching scenario, when temperature is increased, diffusion of molecules occurs at a faster rate, leading to the ongoing interactions between the quencher and the fluorophore. Conversely, in a static quenching scenario, the nonfluorescent ground state complex remains stable with the increasing temperature.

Fluorescence emission spectra of HSA with increasing concentrations of AgNPs were obtained at temperatures ranging from 20 to 60 °C (293–333 K). To determine the mechanism of quenching, the data were analyzed for the quenching constant using the Stern–Volmer eq 1

$$\frac{F_0}{F} = 1 + K_{SV}[Q] \quad (1)$$

where F_0 and F denote the fluorescence intensities in the absence and the presence of the quencher (AgNPs), respectively, [Q] is the concentration of AgNPs, and K_{SV} is the Stern–Volmer quenching constant.[3]

The Stern–Volmer quenching plots for the AgNPs are shown in Figure 4, and the corresponding Stern–Volmer quenching constants are displayed in Tables 1, 2, and S2 (Supporting Information) for Cur-AgNPs, EGCG-AgNPs, and Ct-AgNPs, respectively. The K_{SV} values for Cur-AgNPs show a consistent decrease with the increasing temperature from 30 to 60 °C (Table 1). This indicates that the quenching mechanism is predominantly due to static binding of HSA to Cur-AgNPs because a decrease in K_{SV} with an increasing temperature indicates complex formation or static quenching.[1,3,39] The K_{SV} values for EGCG-AgNPs, on the other hand, decrease only in the 40–60 °C range with the increasing temperature, whereas at a lower temperature range (20–40 °C), an increase in K_{SV} is observed (Table 2). This suggests that at the physiological temperature of 37 °C, EGCG-AgNPs exhibit dynamic quenching. However, as temperature increases, there is an evidence of static quenching. Notably, even in the case of Cur-AgNPs, an increase in K_{SV} indicative of dynamic quenching is observed at lower temperatures (20–30 °C). The comparisons between two phytochemical-coated AgNPs at the physiological temperature suggests that Cur-AgNPs interact more strongly with HSA through a static complex formation, in contrast to EGCG-AgNPs, whose interactions with HSA are less stable because of dynamic interactions. In contrast to phytochemical-

DOI: 10.1021/acsomega.7b01878
ACS Omega 2018, 3, 2220–2229

coated AgNPs, citrate-capped NPs show dynamic interactions with HSA across the wider temperature range of 20−60 °C.

Further extension of the Stern−Volmer equation allows calculation of the biomolecular quenching rate constant (k_q) as shown in eq 2

$$\frac{F_0}{F} = 1 + K_{SV}[Q] = 1 + k_q\tau_0[Q] \quad (2)$$

where K_{SV} is the Stern−Volmer quenching constant, k_q is the biomolecular quenching rate constant, and τ_0 is the average lifetime of the fluorophore without the quencher. F_0 and F denote the fluorescence intensities in the absence and the presence of the quencher (AgNPs), respectively, whereas [Q] is the concentration of AgNPs.[3]

The fluorescence lifetime of the HSA is 10^{-8} s (τ_0)[3], and k_q is calculated using the formula K_{SV}/τ_0. In the case of dynamic quenching, the maximum possible scatter quenching collision constant of various quenchers with the biopolymer is 2.0×10^{10} M^{-1} s^{-1}.[3,18] The k_q values obtained for all the three NPs are in the order of 10^{13} M^{-1} s^{-1} (Tables 1 and 2 and Supporting Information Table S2), which are 3 orders of magnitude higher over the diffusion-controlled values encountered during dynamic interactions. This implies that at least to a finite extent, the AgNP−HSA complex is formed in the case of all NPs, leading to a degree of static interactions.[11] The Cur-AgNPs show the highest k_q values, followed by EGCG-AgNPs and Ct-AgNPs, suggesting that the degree of static interactions between AgNPs and HSA is the largest in the case of Cur-AgNPs. Similarly, the K_{SV} values also indicated that the contribution of the static interactions was the largest in Cur-AgNPs (30−60 °C), followed by EGCG-AgNPs (40−60 °C), whereas Ct-AgNPs did not show evidence of static interactions. These studies, in combination, suggest that phytochemical-coated AgNPs show a complex interplay between dynamic and static interactions with HSA, such that interactions of HSA with Cur-AgNPs seem to be significantly stronger than those with EGCG-AgNPs.

Binding Constant and Thermodynamic Parameters. The double logarithmic regression curves of $\log[(F_0 - F)/F]$ versus $\log[Q]$ were plotted for the AgNPs, the intercept of which gives K, the binding constant (Supporting Information Figure S4). These binding constants are shown in Tables 1, 2, and S2 (Supporting Information) for Cur-AgNPs, EGCG-AgNPs, and Ct-AgNPs, respectively. The K value for Ct-AgNPs shows an increase with the temperature, indicating that the binding capacity increases as the temperature rises, and a similar observation has been made previously in the case of BSA interactions with citrate-capped AgNPs.[3] The value of K decreases with the increasing temperature for both the phytochemical-coated AgNPs, and this indicates a reduction in binding capacity with a concomitant rise in the temperature. Despite the K_d values (Figure 3D) indicating high affinity of Cur-AgNPs and EGCG-AgNPs toward HSA, the decrease in the binding constant with temperature signifies the instability of the AgNPs−HSA complex in these cases.[39,40]

To determine the thermodynamic forces and the nature of binding of AgNPs to HSA, van't Hoff plots were used (Supporting Information, Figure S5). Because Ct-AgNPs exhibited a linear van't Hoff plot (Figure S5A), the changes in enthalpy and entropy were determined using the following equation

$$\ln K = \frac{-\Delta H^\circ}{RT} + \frac{\Delta S^\circ}{R} \quad (3)$$

where K is the binding constant at the corresponding temperature (T) in Kelvin; R is the gas constant (8.314 J K^{-1} mol^{-1}); and ΔH° and ΔS° correspond to the changes in enthalpy and entropy, respectively.[3] However, because the trend for Cur-AgNPs and EGCG-AgNPs (Figure S5B,C) deviated from the linear dependence, polynomial equations were utilized as described previously.[41] The dependence of ln K on $1/T$ can be reduced to the quadratic form with three parameters (α_0, α_1, and α_2), which is represented in a polynomial equation as follows

$$\ln K = \alpha_0 + \frac{\alpha_1}{T} + \frac{\alpha_2}{T^2} \quad (4)$$

Using these regression parameters, the thermodynamic parameters were calculated using the following equations[41]

$$\Delta H^\circ = -R\left(\alpha_1 + 2\frac{\alpha_2}{T}\right) \quad (5)$$

$$\Delta S^\circ = R\left(\alpha_0 - \frac{\alpha_2}{T^2}\right) \quad (6)$$

and the Gibbs free energy (ΔG°) was determined using the equation

$$\Delta G^\circ = \Delta H^\circ - T\Delta S^\circ \quad (7)$$

The nature of interactions between HSA and AgNPs can be determined from the changes in the enthalpy and entropy of the overall system. When ΔH° and ΔS° are both less than zero, such systems are dominated with van der Waals forces and hydrogen bonds; when ΔH° and ΔS° are both greater than 0, this is characteristic of a system rich in hydrophobic forces; whereas when $\Delta H^\circ < 0$ and $\Delta S^\circ > 0$, this represents the system stabilized by electrostatic forces.[3,18] Negative ΔG° values indicate a spontaneous and thermodynamically favorable process.[3,18] As such, the thermodynamic parameters obtained for Cur-AgNPs, EGCG-AgNPs, and Ct-AgNPs are displayed in Tables 1 and 2, and in Supporting Information Table S2, respectively. On the basis of these thermodynamic parameters, both the phytochemical-coated AgNPs exhibit hydrophobic interactions with HSA, and these interactions are thermodynamically favorable at ambient temperatures. However, with the increasing temperature, the interactions lose their spontaneity (positive ΔG°), and the van der Waals and hydrogen bonding start playing the major role in AgNP−HSA interactions. Pristine phytochemicals have also been previously observed to interact with HSA through van der Waals forces and hydrogen bonds,[12,37] indicating that as the interaction temperature increases, the phytochemicals bound onto the NP surface obtain a greater degree of freedom to interact with the serum proteins in a manner that they interact in their free states. This also affirms that the surface coatings of NPs do play an important role in determining their interactions with the serum proteins. In contrast, Ct-AgNPs without any phytochemical coating (Supporting Information, Table S2) show a consistent behavior across a broader temperature range, which support a spontaneous thermodynamically favourable interaction with HSA molecules dominated by hydrophobic forces. This observation is in line with previous studies on citrate-capped NPs.[3] Overall, a comparison between citrate- and phytochemicals-coated AgNPs suggests that while the latter do bind to

DOI: 10.1021/acsomega.7b01878
ACS Omega 2018, 3, 2220−2229

HSA, the binding is less favorable than the interactions between Ct-AgNPs and HSA.

Effect of AgNPs on the Secondary Structure of HSA. Circular dichroism (CD) spectroscopy provides a convenient method for assessing the changes in the secondary structure, conformation, and stability of proteins in solution on interaction with NPs. Typically, the α-helices of proteins exhibit two negative bands at 208 and 222 nm, contributed by the $\pi-\pi^*$ and $n-\pi^*$ transitions of the peptide bonds of the α-helix, respectively.[1,40] The CD spectra of HSA in the presence and absence of AgNPs are shown in Figure 5. The α-helix was

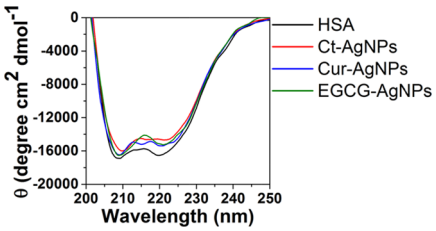

Figure 5. CD spectra of HSA in the absence and the presence of the AgNPs.

calculated from the mean residue ellipticity (MRE) values at 208 nm using the following equation

$$\text{MRE} = \frac{\text{observed CD (mdeg)}}{C_p n l \times 10} \quad (8)$$

where C_p is the molar concentration of the protein, n is the number of amino acid residues in HSA (585), and l is the path length (0.1 cm).[40] The percentage of α-helix content was calculated using the equation

$$\alpha\text{-helix (\%)} = \frac{-\text{MRE}_{208} - 4000}{33\,000 - 4000} \times 10 \quad (9)$$

where MRE_{208} is the observed MRE at 208 nm, 4000 is the MRE of the β-form and random coil conformation cross at 208 nm, and 33 000 is the MRE value of a pure α-helix at 208 nm.[40]

The α-helix content, as obtained from CD spectroscopy of HSA in the phosphate buffer, showed a reduction from 44.4% in the case of free HSA to 38.6, 41.8, and 42.4% in the presence of Ct-AgNPs, Cur-AgNPs, and EGCG-AgNPs, respectively. This indicates that while all three AgNPs show a reduction in the α-helices content of HSA, the reduction with Ct-AgNPs was the greatest. Between the two phytochemical-coated AgNPs, Cur-AgNPs showed greater reduction than EGCG-AgNPs. The CD spectroscopy studies, therefore, support the fact that the interaction of phytochemical-coated AgNPs with human serum proteins causes fewer changes in the secondary structure of the protein, compared to citrate-stabilized AgNPs.

CONCLUSIONS

Citrate and sodium borohydride are the commonly employed reducing agents to prepare metal NPs of gold and silver. In comparison, while the use of phytochemicals to prepare metal NPs is not a common practice, the antioxidant capability of a large group of phytochemicals offers remarkable potential in their utility as "soft" reducing agents for metal NP synthesis. The inherent biocompatibility of a large number of these phytochemicals also has the potential to employ phytochemical-coated NPs for a myriad of biomedical applications. It is acknowledged that the interaction of sodium borohydride or citrate-capped metal NPs with serum proteins has been widely studied, and that most of these studies have focussed on BSA.[1,3,16] There have been a selected few studies involving phytochemicals; however, these studies have employed the whole plant extracts for NP synthesis without using individual phytochemicals.[11,15] These studies involving plant extracts for NP production do not provide molecular-level interaction insights and may lack the necessary aspects of quality control and precision manufacturing required for the intended biomedical use. Therefore, this study has, for the first time, obtained new insights into the human serum protein interactions of two phytochemical-stabilized metal NPs (Cur-AgNPs and EGCG-AgNPs) while comparing their performance with the widely reported Ct-AgNPs.

One of the key findings of our study is that the investigated phytochemical-capped AgNPs initially interact with HSA more strongly compared to Ct-AgNPs; however, the resultant NP–HSA complexes subsequently become less stable in the case of the former, which causes a lesser degree of changes in the protein conformation during interactions. Another key difference observed between these two groups of AgNPs is that while under ambient conditions, all three types of AgNPs interacted with HSA predominantly via hydrophobic forces; however, with increasing temperatures (including at the physiological temperature), phytochemical-stabilized AgNPs showed a shift toward van der Waals and H-bonding interactions. If compared within the phytochemical-capped group of AgNPs, while Cur-AgNPs showed static interactions with HSA, the EGCG-AgNPs interacted in a dynamic fashion. The outcomes of our study reveal that the use of phytochemicals as NP surface ligands offers new opportunities in controlling the interaction of NPs with complex biological fluids. For instance, differential interactions of different surface coatings of NPs with serum proteins have already been explored for developing "chemical nose-tongue" sensors.[8] It is also noted that the formation of a PC once a NP comes in contact with biological fluids is a highly complex process. The current study focussed on understanding the interaction of phytochemical-coated NPs with HSA provides only a guiding tool, suggesting the potential benefits of phytochemicals in controlling the formation of a PC. However, further studies involving interactions of these NPs with complex fluids and full plasma will need to be performed to obtain a more comprehensive understanding of these interactions. Overall, the natural access to a repertoire of phytochemical molecules with diverse functional groups is likely to offer new opportunities in the field of nanodiagnostics and nanomedicine.

MATERIALS & METHODS

Materials. Silver sulphate (Ag_2SO_4), silver nitrate ($AgNO_3$) curcumin, EGCG, potassium hydroxide (KOH), HSA, monosodium phosphate (NaH_2PO_4), disodium phosphate (Na_2HPO_4), and dialysis membrane (12 kDa molecular weight cutoff) were purchased from Sigma-Aldrich (Castle Hill, NSW, Australia). A dialysis membrane was used after sensitizing by boiling in distilled water. All other materials were used as purchased without further modification. Sodium phosphate buffer (pH 7.4) was prepared by mixing 40.5 mL of 0.2 M Na_2HPO_4 with 9.5 mL of 0.2 M NaH_2PO_4 and made up to a final volume of 100 mL. Deionized Milli-Q water was used for all experiments.

AgNP Synthesis. The citrate-capped AgNPs (Ct-AgNPs) were synthesized using the citrate reduction method. Silver

DOI: 10.1021/acsomega.7b01878
ACS Omega 2018, 3, 2220–2229

nitrate (100 mL, 10 mM) was heated on a magnetic stirrer to 95 °C, and 2 mL of 1% trisodium citrate solution was added. The method of synthesis of curcumin-reduced AgNPs (Cur-AgNPs) and EGCG-reduced AgNPs (EGCG-AgNPs) was adapted from Selvakannan et al.[23] To synthesize Cur-AgNPs, curcumin was dissolved in 0.1 M KOH and added to boiling water with equimolar aqueous silver sulphate solution. EGCG-AgNPs were similarly prepared by adding equimolar concentrations of aqueous silver sulphate and EGCG solutions followed by 0.1 M KOH. Heating was continued until the solutions turned yellowish brown, signifying the formation of AgNPs. The AgNPs were rotary-evaporated at 70 hPa, with the water bath heated to 70 °C and concentrated approximately to 10 times of the original concentration. The concentrated solutions were dialyzed for 24 h against deionized water at room temperature to remove excess KOH, unreduced metal ions, and/or unbound molecules, if any.

Characterization of NPs. Synthesized AgNPs were characterized by UV−vis spectroscopy using a Varian Cary 50 spectrophotometer (Australia) from 200 to 800 nm in a quartz cuvette with a path length of 1 cm. The nanoparticle core size was assessed by TEM. TEM images were obtained by drop-casting the dialyzed samples on carbon-coated copper grids and imaged using the JEOL 1010 TEM (USA) instrument operated at 100 kV. The hydrodynamic diameter and zeta potential of NPs were measured using a Malvern Nano-Zetasizer (UK) at 25 °C. The samples were loaded into a folded capillary cell for the zeta potential measurements. The Smoluchowski methodology for aqueous media was employed, and a maximum of 100 runs was performed.[42] For DLS, the samples were loaded into a polystyrene cuvette of 1 cm path length. For HSA−AgNP interaction studies, the molar equivalent concentration of Ag in AgNPs was determined by atomic absorption spectroscopy using a Varian PerkinElmer atomic absorption spectrometer. Throughout this study, the indicated AgNP concentration corresponds to the molar equivalent of Ag^+ ions.

Interaction of AgNPs with HSA. To study the interaction of the phytochemical-coated AgNPs with HSA, concentration-dependent studies were performed by incubating varying concentrations of the AgNPs (0.1−240 μM) with 3 μM of HSA in sodium phosphate buffer for 2 h at 4 °C. All solutions were brought to room temperature for 30 min before acquiring UV−visible absorbance and fluorescence spectra. Fluorescence measurements were performed on a Jobin Yvon HORIBA FluoroMax 4 spectrophotometer (Japan). Because tryptophan is excited at 295 nm and produces an emission peak between 300 and 500 nm,[26] fluorescence spectra were recorded in the range of 300−500 nm by exciting the reaction mixture at 295 nm at room temperature.

Further, to determine the binding affinity of AgNPs to HSA using the fluorescence spectra, the dissociation constant (K_d) was determined using eq 10

$$Y = \frac{B_{max}X}{K_d + X} \tag{10}$$

where B_{max} refers to the binding maxima and X and Y refer to the corresponding values from the X and Y axes.[26] This equation was fitted using GraphPad Prism 7.02, GraphPad, La Jolla, CA.

For temperature-dependent studies, fluorescence spectra were collected from 20 to 70 °C at intervals of 10 °C. From these data, the binding mechanism was elucidated using Stern−Volmer plots by plotting F_0/F versus [Q] at different temperatures.[43] The binding constant and the number of binding sites were determined using eq 11

$$\log \frac{F_0 - F}{F} = \log K + n \log[Q] \tag{11}$$

where F_0 and F denote the fluorescence intensities in the absence and the presence of the quencher (AgNPs), respectively. [Q] is the concentration of the AgNPs, K is the binding constant, and n is the number of binding sites.[3] Because the response of AgNPs at higher concentrations deviated from linearity, only low concentrations of AgNPs were used for calculations.

CD Spectroscopy. The conformational changes to HSA on interactions with the AgNPs were studied using a Jasco J-815 spectropolarimeter (USA) at room temperature (25 °C). The path length of the quartz cell used was 0.1 cm. The protein concentration was 3 μM, and the AgNP concentration was 240 μM. The CD spectra were collected from 190 to 300 nm using a scan speed of 50 nm/min under a constant nitrogen flow. Three scans were averaged to improve the signal to noise ratio. The ellipticity values are expressed in terms of mean residue molar ellipticity (θ) in degree cm^2 $dmol^{-1}$. Appropriate baseline corrections using sodium phosphate buffer were made.

■ ASSOCIATED CONTENT

Supporting Information

The Supporting Information is available free of charge on the ACS Publications website at DOI: 10.1021/acsomega.7b01878.

UV−visible absorption spectra of trisodium citrate, curcumin, and EGCG; nanoparticles size and zeta potential measurements; Stern−Volmer constants and thermodynamic parameters for Ct-AgNPs; fluorescent spectra of HSA in the presence of methanol and ethanol; FTIR spectra of the Cur-AgNPs and EGCG-AgNPs; double logarithmic regression plots of $\log[(F_0 - F)/F]$ versus log[Q]; and van't Hoff plots (PDF)

■ AUTHOR INFORMATION

Corresponding Authors

*E-mail: vipul.bansal@rmit.edu.au. Phone: +61 3 9925 2121. Fax: +61 3 9925 3747 (V.B.).

*E-mail: ravi.shukla@rmit.edu.au. Phone: +61 3 992529070. Fax: +61 3 99253747 (R.S.).

ORCID

Vipul Bansal: 0000-0002-3354-4317

Author Contributions

The manuscript was written through contributions of all authors. All authors have given approval to the final version of the manuscript. A.N.A. performed the experiments; V.B. and R.S. designed the study; all authors jointly analyzed the data and wrote the manuscript.

Notes

The authors declare no competing financial interest.

■ ACKNOWLEDGMENTS

A.N.A. acknowledges the Australian Technology Network for a Ph.D. scholarship support. R.S. acknowledges the Maxwell Eagle endowment fund. T.K.S. thanks the Commonwealth of Australia for an Endeavour Research Award for spending a research period at RMIT University. The authors acknowledge

DOI: 10.1021/acsomega.7b01878
ACS Omega 2018, 3, 2220−2229

the Australian Research Council for fellowship and funding support (LP130100437—V.B. and R.S.; FT140101285—V.B.; DP170103477—V.B.). V.B. acknowledges the generous support of Ian Potter Foundation in establishing Sir Ian Potter NanoBioSensing Facility at RMIT University. Authors acknowledge the support from the RMIT Micro Nano Research Facility (MNRF) and RMIT Microscopy and Microanalysis Facility (RMMF) for technical assistance and providing access to characterization facilities.

■ ABBREVIATIONS

EGCG, epigallocatechin gallate; Cur, curcumin; HSA, human serum albumin; BSA, bovine serum albumin; AgNP, silver nanoparticle

■ REFERENCES

(1) Zhang, W.; Zhang, Q.; Wang, F.; Yuan, L.; Xu, Z.; Jiang, F.; Liu, Y. Comparison of interactions between human serum albumin and silver nanoparticles of different sizes using spectroscopic methods. *Luminescence* **2015**, *30*, 397−404.

(2) Manivel, A.; Anandan, S. Spectral interaction between silica coated silver nanoparticles and serum albumins. *Colloids Surf., A* **2012**, *395*, 38−45.

(3) Mariam, J.; Dongre, P. M.; Kothari, D. C. Study of Interaction of Silver Nanoparticles with Bovine Serum Albumin Using Fluorescence Spectroscopy. *J. Fluoresc.* **2011**, *21*, 2193−2199.

(4) Lundqvist, M.; Stigler, J.; Elia, G.; Lynch, I.; Cedervall, T.; Dawson, K. A. Nanoparticle size and surface properties determine the protein corona with possible implications for biological impacts. *Proc. Natl. Acad. Sci. U.S.A.* **2008**, *105*, 14265−14270.

(5) Carnovale, C.; Bryant, G.; Shukla, R.; Bansal, V. Size, shape and surface chemistry of nano-gold dictate its cellular interactions, uptake and toxicity. *Prog. Mater. Sci.* **2016**, *83*, 152−190.

(6) Boulos, S. P.; Davis, T. A.; Yang, J. A.; Lohse, S. E.; Alkilany, A. M.; Holland, L. A.; Murphy, C. J. Nanoparticle-protein interactions: a thermodynamic and kinetic study of the adsorption of bovine serum albumin to gold nanoparticle surfaces. *Langmuir* **2013**, *29*, 14984−14996.

(7) Selva Sharma, A.; Ilanchelian, M. Comprehensive Multi-spectroscopic Analysis on the Interaction and Corona Formation of Human Serum Albumin with Gold/Silver Alloy Nanoparticles. *J. Phys. Chem. B* **2015**, *119*, 9461−9476.

(8) De, M.; Rana, S.; Akpinar, H.; Miranda, O. R.; Arvizo, R. R.; Bunz, U. H. F.; Rotello, V. M. Sensing of proteins in human serum using conjugates of nanoparticles and green fluorescent protein. *Nat. Chem.* **2009**, *1*, 461−465.

(9) Shaw, A. K.; Pal, S. K. Spectroscopic studies on the effect of temperature on pH-induced folded states of human serum albumin. *J. Photochem. Photobiol., B* **2008**, *90*, 69−77.

(10) Canoa, P.; Simón-Vázquez, R.; Popplewell, J.; González-Fernández, A. A quantitative binding study of fibrinogen and human serum albumin to metal oxide nanoparticles by surface plasmon resonance. *Biosens. Bioelectron.* **2015**, *74*, 376−383.

(11) Ambika, S.; Sundrarajan, M. Green biosynthesis of ZnO nanoparticles using Vitex negundo L. extract: Spectroscopic investigation of interaction between ZnO nanoparticles and human serum albumin. *J. Photochem. Photobiol., B* **2015**, *149*, 143−148.

(12) Patra, D.; Barakat, C.; Tafech, R. M. Study on effect of lipophilic curcumin on sub-domain IIA site of human serum albumin during unfolded and refolded states: A synchronous fluorescence spectroscopic study. *Colloids Surf., B* **2012**, *94*, 354−361.

(13) Carril, M.; Padro, D.; del Pino, P.; Carrillo-Carrion, C.; Gallego, M.; Parak, W. J. In situ detection of the protein corona in complex environments. *Nat. Commun.* **2017**, *8*, 1542.

(14) Lo Giudice, M. C.; Herda, L. M.; Polo, E.; Dawson, K. A. In situ characterization of nanoparticle biomolecular interactions in complex biological media by flow cytometry. *Nat. Commun.* **2016**, *7*, 13475.

(15) Yue, H.-L.; Hu, Y.-J.; Chen, J.; Bai, A.-M.; Ouyang, Y. Green synthesis and physical characterization of Au nanoparticles and their interaction with bovine serum albumin. *Colloids Surf., B* **2014**, *122*, 107−114.

(16) Brewer, S. H.; Glomm, W. R.; Johnson, M. C.; Knag, M. K.; Franzen, S. Probing BSA binding to citrate-coated gold nanoparticles and surfaces. *Langmuir* **2005**, *21*, 9303−9307.

(17) Mandal, S.; Hossain, M.; Devi, P. S.; Kumar, G. S.; Chaudhuri, K. Interaction of carbon nanoparticles to serum albumin: elucidation of the extent of perturbation of serum albumin conformations and thermodynamical parameters. *J. Hazard. Mater.* **2013**, *248−249*, 238−245.

(18) Markarian, S. A.; Aznauryan, M. G. Study on the interaction between isoniazid and bovine serum albumin by fluorescence spectroscopy: the effect of dimethylsulfoxide. *Mol. Biol. Rep.* **2012**, *39*, 7559−7567.

(19) Gelamo, E. L.; Tabak, M. Spectroscopic studies on the interaction of bovine (BSA) and human (HSA) serum albumins with ionic surfactants. *Spectrochim. Acta, Part A* **2000**, *56*, 2255−2271.

(20) Singh, D. V.; Bharti, S. K.; Agarwal, S.; Roy, R.; Misra, K. Study of interaction of human serum albumin with curcumin by NMR and docking. *J. Mol. Model.* **2014**, *20*, 2365.

(21) Li, M.; Hagerman, A. E. Role of the flavan-3-ol and galloyl moieties in the interaction of (-)-epigallocatechin gallate with serum albumin. *J. Agric. Food Chem.* **2014**, *62*, 3768−3775.

(22) Liu, S.; Guo, C.; Guo, Y.; Yu, H.; Greenaway, F.; Sun, M. Z. Comparative binding affinities of flavonoid phytochemicals with bovine serum albumin. *Iran. J. Pharm. Res.* **2014**, *13*, 1019−1028.

(23) Selvakannan, P. R.; Swami, A.; Srisathiyanarayanan, D.; Shirude, P. S.; Pasricha, R.; Mandale, A. B.; Sastry, M. Synthesis of aqueous Au core-Ag shell nanoparticles using tyrosine as a pH-dependent reducing agent and assembling phase-transferred silver nanoparticles at the air-water interface. *Langmuir* **2004**, *20*, 7825−7836.

(24) Shukla, R.; Chanda, N.; Zambre, A.; Upendran, A.; Katti, K.; Kulkarni, R. R.; Nune, S. K.; Casteel, S. W.; Smith, C. J.; Vimal, J.; Boote, E.; Robertson, J. D.; Kan, P.; Engelbrecht, H.; Watkinson, L. D.; Carmack, T. L.; Lever, J. R.; Cutler, C. S.; Caldwell, C.; Kannan, R.; Katti, K. V. Laminin receptor specific therapeutic gold nanoparticles (198AuNP-EGCg) show efficacy in treating prostate cancer. *Proc. Natl. Acad. Sci. U.S.A.* **2012**, *109*, 12426−12431.

(25) Yallapu, M. M.; Nagesh, P. K. B.; Jaggi, M.; Chauhan, S. C. Therapeutic Applications of Curcumin Nanoformulations. *AAPS J.* **2015**, *17*, 1341−1356.

(26) Sharma, T. K.; Sapra, M.; Chopra, A.; Sharma, R.; Patil, S. D.; Malik, R. K.; Pathania, R.; Navani, N. K. Interaction of Bacteriocin-Capped Silver Nanoparticles with Food Pathogens and Their Antibacterial Effect. *Int. J. Green Nanotechnol.* **2012**, *4*, 93−110.

(27) Rodrigues, M. A.; Fernandes, J. N.; Ruggiero, R.; Guerra, W. Palladium Complex Containing Curcumin as Ligand: Thermal and Spectral Characterization. *Am. J. Chem.* **2012**, *2*, 157−159.

(28) Snitsarev, V.; Young, M. N.; Miller, R. M. S.; Rotella, D. P. The Spectral Properties of (-)-Epigallocatechin 3-O-Gallate (EGCG) Fluorescence in Different Solvents: Dependence on Solvent Polarity. *PLoS One* **2013**, *8*, No. e79834.

(29) Krukowski, S.; Karasiewicz, M.; Kolodziejski, W. Convenient UV-spectrophotometric determination of citrates in aqueous solutions with applications in the pharmaceutical analysis of oral electrolyte formulations. *J. Food Drug Anal.* **2017**, *25*, 717−722.

(30) Salatin, S.; Maleki Dizaj, S.; Yari Khosroushahi, A. Effect of the surface modification, size, and shape on cellular uptake of nanoparticles. *Cell Biol. Int.* **2015**, *39*, 881−890.

(31) Huang, S.; Qiu, H.; Lu, S.; Zhu, F.; Xiao, Q. Study on the molecular interaction of graphene quantum dots with human serum albumin: combined spectroscopic and electrochemical approaches. *J. Hazard. Mater.* **2015**, *285*, 18−26.

(32) Kim, C.; Savizky, R. M. A fluorescence quenching study of the human serum albumin-quercetin complex by addition of Copper(II), Nickel(II), and Manganese(II). *Res. J. Pharm., Biol. Chem. Sci.* **2013**, *4*, 765−795.

DOI: 10.1021/acsomega.7b01878
ACS Omega 2018, 3, 2220−2229

(33) Röcker, C.; Pötzl, M.; Zhang, F.; Parak, W. J.; Nienhaus, G. U. A quantitative fluorescence study of protein monolayer formation on colloidal nanoparticles. *Nat. Nanotechnol.* **2009**, *4*, 577.
(34) del Pino, P.; Pelaz, B.; Zhang, Q.; Maffre, P.; Nienhaus, G. U.; Parak, W. J. Protein corona formation around nanoparticles—from the past to the future. *Mater. Horiz.* **2014**, *1*, 301−313.
(35) Pelaz, B.; del Pino, P.; Maffre, P.; Hartmann, R.; Gallego, M.; Rivera-Fernández, S.; de la Fuente, J. M.; Nienhaus, G. U.; Parak, W. J. Surface Functionalization of Nanoparticles with Polyethylene Glycol: Effects on Protein Adsorption and Cellular Uptake. *ACS Nano* **2015**, *9*, 6996−7008.
(36) Barik, A.; Mishra, B.; Kunwar, A.; Indira Priyadarsini, K. Interaction of curcumin with human serum albumin: Thermodynamic properties, fluorescence energy transfer and denaturation effects. *Chem. Phys. Lett.* **2007**, *436*, 239−243.
(37) Maiti, T. K.; Ghosh, K. S.; Dasgupta, S. Interaction of (-)-epigallocatechin-3-gallate with human serum albumin: fluorescence, fourier transform infrared, circular dichroism, and docking studies. *Proteins: Struct., Funct., Bioinf.* **2006**, *64*, 355−362.
(38) Ishii, T.; Ichikawa, T.; Minoda, K.; Kusaka, K.; Ito, S.; Suzuki, Y.; Akagawa, M.; Mochizuki, K.; Goda, T.; Nakayama, T. Human serum albumin as an antioxidant in the oxidation of (-)-epigallocatechin gallate: participation of reversible covalent binding for interaction and stabilization. *Biosci., Biotechnol., Biochem.* **2011**, *75*, 100−106.
(39) Ambika, S.; Sundrarajan, M. Green biosynthesis of ZnO nanoparticles using Vitex negundo L. extract: Spectroscopic investigation of interaction between ZnO nanoparticles and human serum albumin. *J. Photochem. Photobiol., B* **2015**, *149*, 143−148.
(40) Yue, H.-L.; Hu, Y.-J.; Chen, J.; Bai, A.-M.; Ouyang, Y. Green synthesis and physical characterization of Au nanoparticles and their interaction with bovine serum albumin. *Colloids Surf., B* **2014**, *122*, 107−114.
(41) Galaon, T.; David, V. Deviation from van't Hoff dependence in RP-LC induced by tautomeric interconversion observed for four compounds. *J. Sep. Sci.* **2011**, *34*, 1423−1428.
(42) Munusamy, P.; Wang, C.; Engelhard, M. H.; Baer, D. R.; Smith, J. N.; Liu, C.; Kodali, V.; Thrall, B. D.; Chen, S.; Porter, A. E.; Ryan, M. P. Comparison of 20 nm silver nanoparticles synthesized with and without a gold core: Structure, dissolution in cell culture media, and biological impact on macrophages. *Biointerphases* **2015**, *10*, 031003.
(43) Quenching of Fluorescence. In *Principles of Fluorescence Spectroscopy*; Lakowicz, J., Ed.; Springer US, 2006; pp 277−330.

DOI: 10.1021/acsomega.7b01878
ACS Omega 2018, 3, 2220−2229